Inorganica Chimica Acta, *202* (1992) 241–251

Assignment of heme resonances in the ^{1}H NMR spectrum of oxidized *Desulfovibrio vulgaris* (Hildenborough) cytochrome c_3

Marco Sola*

Department of Chemistry, University of Modena, via Campi 183, 41100 Modena (Italy)

and James A. Cowan

Department of Chemistry, The Ohio State University, 140 West 18th Avenue, Columbus, OH 43210 (USA)

(Received May 14, 1992; revised July 9, 1992)

Abstract

A combination of 2D COSY and NOESY experiments and 1D nuclear Overhauser effect measurements have allowed an extensive assignment of the hyperfine-shifted heme resonances in the downfield region of the ^{1}H NMR spectrum of the fully oxidized tetraheme cytochrome c_3 from *Desulfovibrio vulgaris*, Hildenborough. Fifteen of the sixteen heme methyl groups were identified and assigned, some on a tentative basis. Most of the one-proton paramagnetic resonances were demonstrated to arise from the α-CH_2 groups of the heme propionate side chains, and from the β-CH_2 groups of the iron-binding axial histidines. Assignment of methyl resonances to individual hemes was achieved by reference to previous calculations of electron density distributions on the four hemes of the highly homologous Miyazaki protein obtained by NMR data (*Biochemistry*, *29* (1990) 2257). The methyl hyperfine shift patterns are apparently different for the individual hemes. Despite the complexity of the system due to interheme interactions, we have determined that these patterns appear to be influenced by the orientation of the imidazole planes of the iron-binding axial histidines, as found for simpler monoheme proteins.

Introduction**

Cytochromes c_3 are a family of low molecular weight ($M_r \sim 13$ kDa) electron-transport proteins that may be isolated from sulfate-reducing bacteria [1, 2]. There is evidence that this cytochrome is a natural redox partner of ferredoxin and hydrogenase, and serves a key role in the major bioenergetic pathways of cellular metabolism. *In vitro* it has been found to interact with ferredoxin, rubredoxin and flavodoxin. The protein is also of intrinsic interest inasmuch as the polypeptide backbone carries four heme units arranged in a variety of orientations that interact with respect to electron exchange, magnetic properties and the regulation of tertiary structure. The size of the protein has facilitated detailed study of its physicochemical properties by a variety of physical techniques. Structural data is available for two cytochromes c_3 isolated from *Desulfovibrio vulgaris* Miyazaki F [3], and *Desulfovibrio desulfuricans* Norway [4, 5], which has facilitated modelling of the interaction of cytochrome c_3 with putative biological redox partners [6–8]. ^{1}H NMR studies dealing with the paramagnetic resonances [9] arising from the four hemes have proved particularly valuable in analyzing the structure and redox properties of the c_3 family, however, detailed assignments have been lacking [7, 10–19]. Recently, 1D-nuclear Overhauser effect experiments on *D. vulgaris* cytochrome c_3, Miyazaky, have allowed a partial assignment of heme methyl signals [18, 20]. In this paper we report an extensive ^{1}H NMR study, through 1D NOE measurements and 2D techniques, of the Hildenborough protein and propose assignments of most of the low-field hyperfine-shifted resonances. Such assignments facilitate the use of NMR to both monitor the interaction of cytochrome c_3 with biological redox partners and analyze the orientation and dynamics of residues defining the heme pocket. The application of 2D NMR methods to paramagnetic proteins has only recently been demonstrated [21–24]. Such methods have been applied mostly to heme proteins where partial assignments had already been established through 1D techniques on proteins reconstituted with isotopically-

*Author to whom correspondence should be addressed.

**The abbreviations used are: NOE, nuclear Overhauser effect; NOESY, two-dimensional nuclear Overhauser effect spectroscopy; COSY, two-dimensional correlation spectroscopy; WEFT, water-eliminated Fourier transform; MODEFT, modified driven equilibrium Fourier transform.

0020-1693/92/$5.00

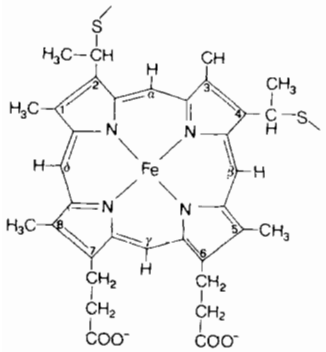

Fig. 1. Structure of the *c*-type cytochrome heme ring system showing the atom numbering.

labeled hemes. Subsequent 2D experiments allowed, in a number of cases, a full assignment of the paramagnetic resonances that were then used to provide structural details of the protein environment around the heme [21–32].

The structure of heme *c* is depicted in Fig. 1. The dipolar connectivities between the 1-CH_3 and the 8-CH_3 groups and those among the propionate side chains in positions 6 and 7 and the 5- and 8-CH_3 groups, respectively, are useful for assignment purposes. The network of connectivities obtained by the 2D NOESY and COSY maps, in conjunction with the X-ray structure of the Miyazaki protein (87% homology with cytochrome c_3 from *D. vulgaris*) (Hildenborough) [33]) and with reference to a partial resonance assignment reported by Fan *et al.* [20], have allowed the assignment of a large number of hyperfine-shifted resonances to groups of individual hemes. A few of these are tentative, due to the absence of any previous firm resonance assignments by use of isotopically labelled hemes.

Experimental

Desulfovibrio vulgaris (Hildenborough, NCIB 8303) was grown in an enriched Baars medium (ATCC medium No. 1249) at the Fermentation Laboratory, Department of Biochemistry, University of Wisconsin. Cytochrome c_3 was purified as described by Tan and Cowan [34]. Monodimensional ^{1}H NMR spectra were obtained on Bruker AMX-400 and Bruker AM-500 spectrometers using 16 K data points over a 40 and 50 kHz spectral bandwidth, respectively. Protein concentrations for NOE measurements were approximately 5 mM in 50 mM sodium phosphate buffer (D_2O, pH 7). Chemical shifts are reported in ppm by assigning a 4.80 ppm value to the residual water peak. Suppression of the residual water signal was achieved with the super-WEFT pulse sequence (180-τ-90-AQ + delay) [35] using recycle times (AQ + delay)of 300–350 ms and delay times (τ) of 170–190 ms. ^{1}H NOE measurements on the hyperfine-shifted resonances [36] were obtained directly with the same sequence by cycling the frequency of the decoupler, kept on during the delay time τ, according to the scheme: $\omega_2-(\omega_2+\delta)-\omega_2-(\omega_2-\delta)$, where ω_2 is the frequency of the irradiated signal and δ the off-resonance offset [37, 38]. On- and off-resonance spectra were automatically subtracted during the sequence by cycling the received phase. The reported spectra were obtained with 30 000–40 000 scans. A line broadening of 10 Hz was used throughout. The large signal-to-noise ratio allowed detection of NOEs as low as 0.4%. The steady-state NOE is the fractional change in the intensity of a given spin when that of a dipole-coupled spin belonging to the same molecule is saturated [39, 40]. For an isolated two-spin system (*ij*) separated by a distance r_{ij} and tumbling with a correlation time τ_c, if a saturating frequency is applied selectively to *j* the steady-state NOE on signal *i* is given by

$$\eta_{ij}=\sigma_{ij}/\rho_i$$

where σ_{ij} is the cross-relaxation rate (proportional to r^{-6}) and ρ_i is the intrinsic spinlattice relaxation rate of *i*. In the absence of local motions, τ_c coincides with the protein tumbling time. The cross-relaxation term allows the internuclear distance to be estimated from NOE measurements. In paramagnetic systems, the large ρ_i values reduce the intensity of the observed NOEs. As a result, a large signal-to-noise is required to detect NOEs that may ne lower than 1%. Such NOEs are all primary, however, since spin-diffusion is quenched [41].

T_1 values were obtained with the MODEFT sequence [42]. A computer-graphics analysis of the X-ray structure of *D. vulgaris* cytochrome c_3 (Miyazaki), which is 87% homologous to the Hildenborough protein [33], was performed with the Sybyl program (by Trypos Associates) on an Evans & Sutherland PS-390 terminal connected with a microVAX data station.

Phase-sensitive NOESY spectra were obtained at 400 MHz on a Bruker AMX-400 spectrometer by using the phase sensitive absorption mode (TPPI) [43]. The residual water peak was suppressed by a decoupler pulse during the relaxation delay and mixing time. Mixing times of 40, 50, 80 and 100 ms were used. The best results, in terms of cross-peak detection, were obtained with a 50 ms mixing time. The data were collected with a 6.2 μs (90°) pulse over a 25 kHz bandwidth with a total recycle time of 613 ms. 2K data points in t_2, and 1024 t_1 increments with 128 scans per t_1 were used. Upon zero filling in the t_1 dimension, the final data matrix was 2K×2K with a digital resolution of 12.2 Hz/point. COSY experiments were carried out with a relaxation delay of 600 ms during which the water signal was suppressed by a presaturation pulse. 512 t_1 increments summing 256 scans per t_1 were

recorded with 1K data points in t_2. The data set were zerofilled to 1K×1K. Data were processed in magnitude mode. Prior to Fourier transformation the 2D data sets were multiplied by a 45 °C (NOESY) or 0° (COSY) phase-shifted sine-bell squared function in both dimensions. Data collection and processing were performed with standard Bruker software.

Results

The paramagnetic region of the 400 MHz ^{1}H NMR spectrum of *D. vulgaris* cytochrome c_3 is shown in Fig. 2. Upper and lower case letters are used to denote methyl and one-proton resonances, respectively. The spectral parameters of the hyperfine-shifted signals are listed in Table 1. Care was taken in the measurement of signal intensities: temperature and pH were varied in order to resolve overlapped resonances. Fifteen of the sixteen methyl resonances arising from the methyl groups of the four hemes are observed in the range 31–8 ppm. A group of broad resonances corresponding to seven to eight protons is located in the −10 to −25 ppm region. These resonances were only partially detected in an early report [44], and in general were neglected in the subsequent NMR studies of this protein.

Illustrative examples of the 1D-NOE difference spectra obtained upon saturating in turn all the hyperfine-shifted resonances are reported in Fig. 2 and a map of the NOE connectivities in the paramagnetic region is reported in Table 2. Four connectivities between couples of methyl signals were observed: A–G, B–F, H–J and I–J. Of particular interest is the case of signal

TABLE 1. Assignments for the methyl heme resonances in the ^{1}H NMR spectrum of oxidized cytochrome c_3 (Hildenborough)

Peak	Shift[a]	T_1 (ms)[b]	Assignment
A	30.02	58	8-CH_3 heme I
B	29.73	62	8-CH_3 heme II or III
C	22.52	130	5-CH_3 heme IV
D	22.44	124	3-CH_3 heme IV
E	20.65	26	8- or 5-CH_3 heme II or III
F	18.73	68	1-CH_3 heme II or III
G	18.50	48[c]	1-CH_3 heme I
H	18.42	58[c]	8-CH_3 heme IV
I	17.25	43	5-CH_1 heme I
J	13.82	26	1-CH_3 heme IV
K	10.28	45[c]	3-CH_3 heme I
L	10.10	48[c]	3-CH_3 hemes II and III
M	8.96	–[d]	5- or 8-CH_3 heme II or III, 1-CH_3 heme II or III

[a]Referenced to the residual HDO water peak set to 4.8 ppm. T=298 K. [b]Determined with the MODEFT sequence using different delay times. Estimated error: ±10%. [c]Composite peaks. The errors in T_1 measurements are greater. [d]Bad fit arising from the overlap of fast and slow relaxing resonances.

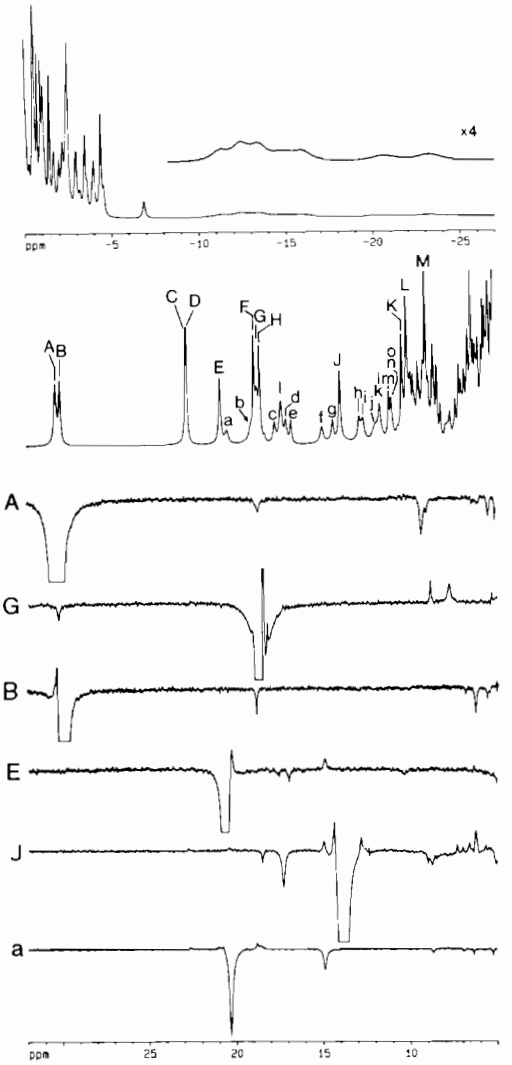

Fig. 2. 400 MHz ^{1}H NMR spectrum of oxidized *D. vulgaris* cytochrome c_3 (Hildenborough) and ^{1}H steady-state NOE difference spectra for some of the downfield shifted hyperfine resonances. The upfield region of the spectrum is reported in the upper part of the Figure and the inset shows the broad resonances in the −10 to −25 ppm region. Letters A to a of the NOE spectra correspond to the irradiated peak. All spectra were obtained in 50 mM sodium phosphate buffer in 99.8% D_2O, pH 7, 298 K. The pH value is not corrected for isotope effects.

J where saturation yields NOEs to two methyl resonances, I and H (Fig. 2, J). The intermethyl distances (4.3±0.3, 4.3±0.3, 4.8±0.3, and 3.4±0.2 Å, respectively) were estimated by use of eqn. (1) and a correlation time of 4.7×10^{-9} s. The first three pairs of resonances most probably correspond to heme 1-CH_3, 8-CH_3 couples, the average distance between such methyl groups being estimated at 5.1 Å [45], while resonances J and I must correspond to two methyl groups close in space belonging to two different hemes.

The 400 MHz NOESY map contains, with only a few exceptions, all the NOE connectivities of the low-

TABLE 2. Nuclear Overhauser effects among the isotropically shifted peaks in oxidized cytochrome c_3 (Hildenborough)[a]

Irradiated peaks	Observed peaks																				
	A	B	C	D	E	F	G	H	I	J	K	L	M	a	c	d	e	f	g	h	i
A							0.7														
B						0.9															
C													0.4							1.3	
D																					
E															0.6	1.2					
F		0.7																			
G	0.8																				
H										(0.1)											
I										1.3											
J								0.4	2.2												
K																					1.0
L																					
M																					
a																		23			
c																34					
d					4.8										36						
e																					
f														25							
g																					
h			9.0										2.0								
i											5.0										

[a]The data are reported as a percent decrease of the signal intensity. Estimated errors are within ±30%.

field hyperfine-shifted resonances observed in the 1D spectra. The downfield portion of the NOESY spectrum in 99.8% D_2O illustrating the cross peaks involving the paramagnetic resonances, and the diamagnetic region of the same spectrum are reported in Fig. 3(A) and (B), respectively. The full COSY map is reported in Fig. 4. Single proton peaks from a to i invariably show a strong NOE (20–50%) and a strong NOESY and COSY cross peak with another one-proton resonance, typical of a methylene couple. In particular, the pairs (h, 6.59), (c, d), (a, f), (b, 7.78), (e, 9.61), (g, 6.18) have been recognized (numerical listings refer to the chemical shift of the geminal resonance falling in the diamagnetic envelope). Each of the first two couples connects with a methyl group (peak C and E, respectively), and so they can be confidently assigned to α-CH_2 groups of heme propionate side chains. Also the other resolved one-proton resonances in the 10.5–11.5 ppm region, except the broad peak j, show at least one very strong NOESY and COSY cross peak.

For the sake of clarity, we will first describe the dipolar and scalar couplings of groups of methyl resonances related by reciprocal NOEs, namely A–G, B–F, and J–H–I, then those of the other CH_3 resonances C, D, E, K, L, and finally the connectivities exhibited by the one-proton resonances.

Couple A–G

The intermethyl contact generates the cross peak 1 in Fig. 3(A). Peak A shows the additional NOESY cross peaks 2–7 involving resonances on the region 9.5 to −1 ppm, while G shows four cross peaks (49–52) with resonances in the range 1.5 to −1 ppm. These connectivities suggest the assignment of peaks A and G to the 8-CH_3 and 1-CH_3 groups of the same heme, respectively. Most of the NOESY cross peaks 2–7 are in fact consistent with the dipolar contacts of an 8-CH_3 group with the propionate chain in position 7. In particular, the following assignment can be proposed: 2 (8-CH_3, 7H$_\alpha$); 3 (8-CH_3, 7H′$_\alpha$); 4 (8-CH_3, 7H$_\beta$); 106 (7H$_\alpha$, 7H′$_\alpha$); 107 (7H$_\alpha$, 7H$_\beta$); 117 (7H′$_\alpha$, 7H$_\beta$). Consistently, the COSY map shows the scalar coupling of the 7H$_\alpha$ proton with its geminal partner (cross peak 23). Cross peaks given by methyl G may arise from the dipolar connectivity of the 1-CH_3 group with the methyl group of the thioether bridge in position 2 and with the methine proton, though the latter usually falls at higher frequencies in *c*-type hemes [46–48]. Methyl peaks, A, G show a common dipolar contact with a resonance at −0.55 ppm (NOESY cross peaks 7 and 52, respectively).

Couple B–F

The intermethyl connectivity is shown by cross peak 8. Cross peaks 9–15 and 41–48 originate from peaks B and F, respectively. Cross peaks 9 and 10 arise from the dipolar contacts of B with protons connected by the strong NOESY and COSY cross peaks 113 and 25, respectively, hence most probably belonging to the α-methylene couple of the propionate chain. No such contacts have been detected for the methyl peak F. Hence B must correspond to the 8-CH_3 group. Assignments of its NOESY cross peaks are: 9(8-CH_3, 7H$_\alpha$); 10 (8-CH_3, 7H′$_\alpha$); 11 (8-CH_3, 7H$_\beta$); 113 (7H$_\alpha$, 7H′$_\alpha$); 114 (7-H$_\alpha$, 7H$_\beta$). The resonances at 2.60, −0.47 and −3.74 ppm show cross peaks with both methyl peaks B and F (12, 42; 14, 46 and 15, 48, respectively). These resonances probably belong to a protein residue close to both the methyl groups, and one of them may correspond to the *δ-meso* proton.

Couples I–J and J–H

The former intermethyl connectivity generates a remarkably strong NOE (Table 2 and Fig. 2, J) and the NOESY cross peak 65. As mentioned above, these two methyl groups are closer than a 1-CH_3, 8-CH_3 couple of the same heme. The X-ray structure shows that the 1-CH_3 group of heme IV and the 5-CH_3 group of heme I are in close contact (methyl carbon distance = 4.17 Å); another interheme methyl distance (methyl 1 of heme II–methyl 5 of heme III) is very similar to a 1-CH_3, 8-CH_3 intraheme distance. It follows that we can reasonably assign the I–J couple to the above short interheme methyl contact. The individual assignments are straightforward: peak J shows an additional weak NOE with methyl H characteristic of a 1-CH_3, 8-CH_3 couple (Fig. 2, J) (the corresponding cross peak is not observed in the NOESY map), hence J corresponds to methyl 1 of heme IV, H to methyl 8 of the same heme, and peak I to methyl 5 of heme I. Most cross peaks given by H and I originate from upfield-shifted resonances and a few of them show a three-proton intensity. Hence they likely correspond to dipole-shifted protons of residues neighboring the hemes. For peaks H and I the only resonances assignable to an α-CH proton of the adjacent propionate chain fall at 4.18 and 6.41 ppm, respectively. The former gives rise to the NOESY cross peak 53 and the latter is observed only at a lower level and is indicated by the open square 76 in Fig. 3(A). Such resonances display several NOEs, but in both cases no COSY cross peaks could be detected, hence their geminal partner could not be identified.

Methyl C

The methyl peak C clearly connects with a propionate α-CH_2 pair formed by resonance h and another one at 6.59 ppm (cross peaks 16 and 18, respectively). The dipolar and scalar contacts among the propionate chain have been almost completely identified. NOESY and

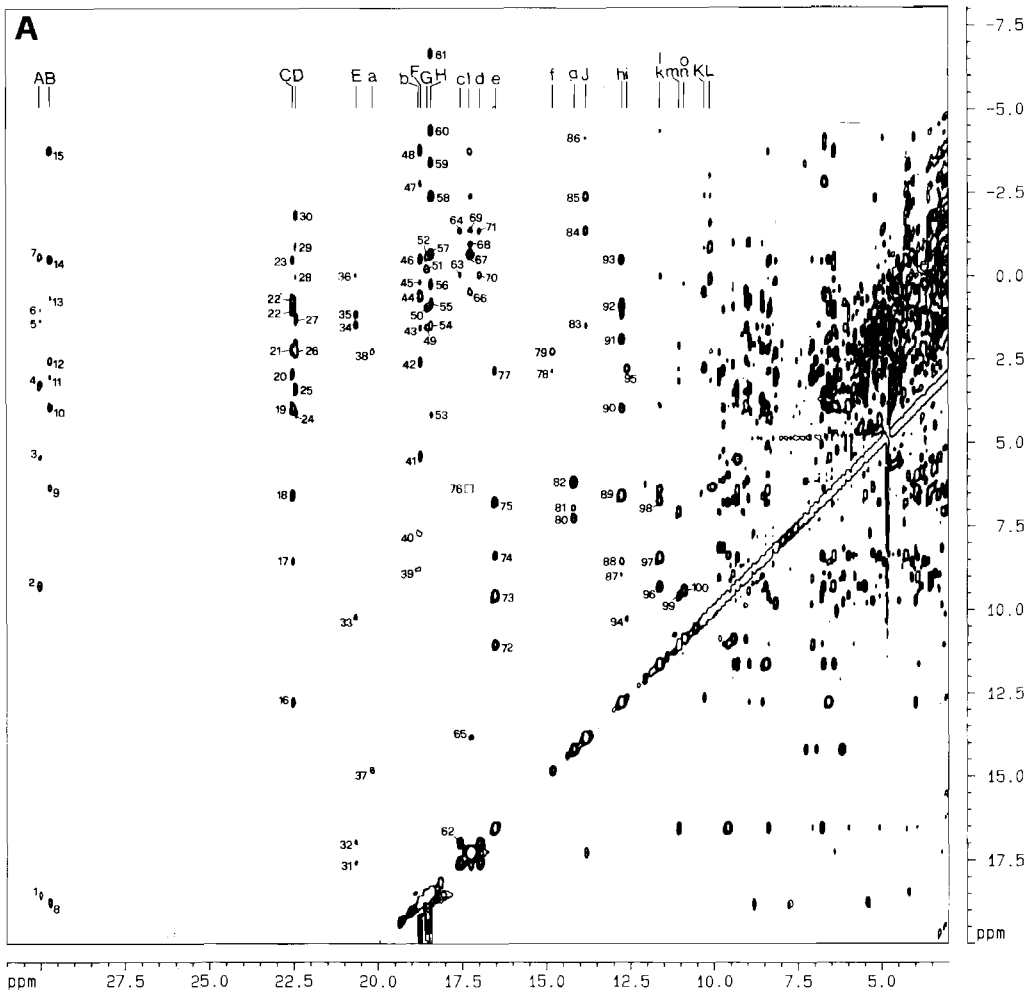

Fig. 3 (For figure legend please see facing page.)

COSY cross peaks can be straigthforwardly assigned as follows (the NOESY peak is reported first): 89, 13 (H_α, H'_α); 92, 14 (H_α, H_β); 93, 15 (H_α, H'_β); 115, 27 (H'_α, H_β); 116, 28 (H'_α, H'_β). Further NOESY cross peaks between C and the propionate chain are: 22 (CH_3, H_β); 23 (CH_3, H'_β). Hencc C is cither a 5- or 8-methyl group. A weak NOE between C and the composite methyl peak M was detected in 1D NOE experiments. Peak M in turn shows connectivities with the components of the above propionate chain (see NOESY cross peaks 87, 108, 109 and 110 between peak M and the above H_α, H'_α, H_β and H'_β protons, respectively). Hence the contact of C with M is likely to involve a one-proton resonance, overlapped to the two-methyl peak, belonging to a residue close to both methyl C and its adjacent propionate side chain. Unfortunately, resonance M could not be satisfactorily resolved in its components by varying temperature and pH. Moreover, it shows further NOESY and COSY cross peaks consistent with the interaction of a heme methyl group with a propionate chain, with the geminal α-CH protons at 3.86 and 1.55 ppm (Table 3), hence is must contain a 5- or 8-CH_3 group.

Methyl E

The observed connectivities with the components of the geminal couple c, d (NOESY cross peaks 31 and 32) indicate that peak E, like methyl C, must belong either to a 5- or an 8-CH_3 group. The following assignments for the NOESY and COSY cross peaks given by E, c and d are straightforward: 31 (CH_3, H_α); 32 (CH_3, H'_α); 36 (CH_3, H_β); 62, 4(H_α, H'_α); 63, 5 (H_α, H_β); 64, 6 (H_α, H'_β); 70, 7 (H'_α, H_β); 71, 8 (H'_α, H'_β); 119, 30 (H_β, H'_β). The remaining NOESY cross peaks 33–35 given by E cannot be assigned with the data available. Variable temperature experiments have shown that the cross peak 33, connecting E with the methyl resonance K, is due to a single proton signal overlapped to the latter methyl peak. 1D NOE experiments indicated that this signal does not connect with another methyl peak, so it cannot be assigned to a *δ-meso* proton.

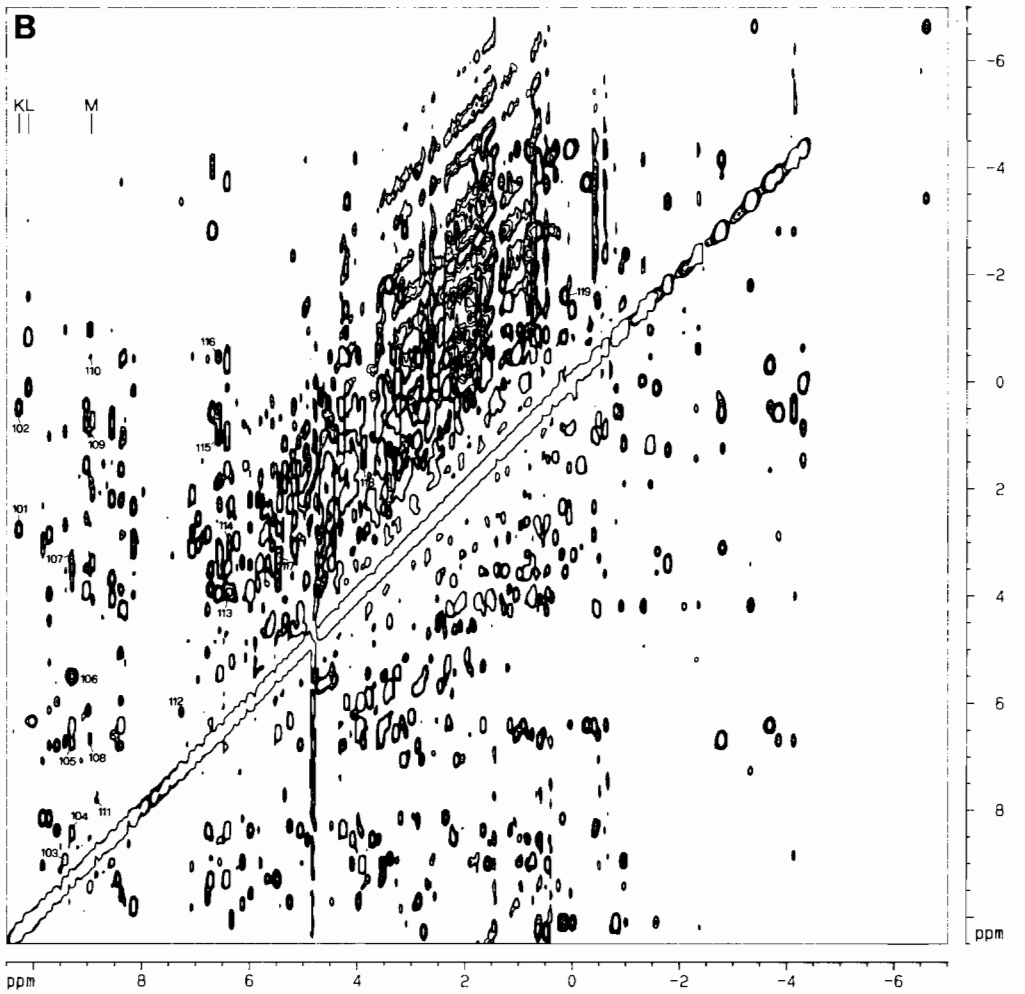

Fig. 3. 400 MHz phase sensitive ^1H NOESY spectrum of oxidized *D. vulgaris* cytochrome c_3 (Hildenborough) in 99.8% D_2O, pH 7, 298 K. (A) Downfield region showing the cross peaks from the hyperfine shifted resonances. (B) Expanded diamagnetic region.

Methyls D and L

These resonances are not involved in 1D-NOE intermethyl connectivities, and no connectivities characteristic of the propionate chain could be detected among the relative cross peaks. Hence peaks D and L are likely to arise from 3-CH_3 groups.

Methyl K

This resonance shows only dipolar contacts with the one-proton signal i and with resonances at 2.7 and 0.48 ppm (NOESY cross peaks 94, 101 and 102, respectively). Though resonances i and that at 2.7 ppm are related by a strong NOESY (cross peak 95), no COSY cross peak could be detected, indicating that they are not the components of a methylene couple. Hence this methyl peak is likely to correspond either to a 1-CH_3 or to a 3-CH_3 group.

From the above data it appears that either methyl C or E must be the fourth 8-CH_3 group whose connectivity with the 1-CH_3 group escaped detection.

One-proton resonances

Five couples of one-proton signals related by strong NOESY and COSY cross peaks could be assigned to α-CH_2 propionate pairs due to the observed connectivity with the adjacent heme methyl group (Table 3). The remaining couples must correspond to dipole-shifted methylene resonances from amino acids close to the hemes, and in particular from β-CH_2 groups of axial histidines, that have been characterized in several low-spin heme proteins [21, 22, 25, 26, 28, 49–52]. Indeed, all the remaining hyperfine-shifted one-proton resonances exhibit dipolar and scalar couplings consistent with the spin system of histidine β-CH_2 and α-CH protons. A list of NOESY and COSY connectivities is reported in Table 4. The pattern of cross peaks generated by the two-proton signal k,l is found consistent with a spin system originating from overlapped β-CHs of two histidines, connected to the geminal partners at 8.48 and 6.75 ppm, that possess α-CH protons both resonating at 9.29 ppm. The NOESY and COSY con-

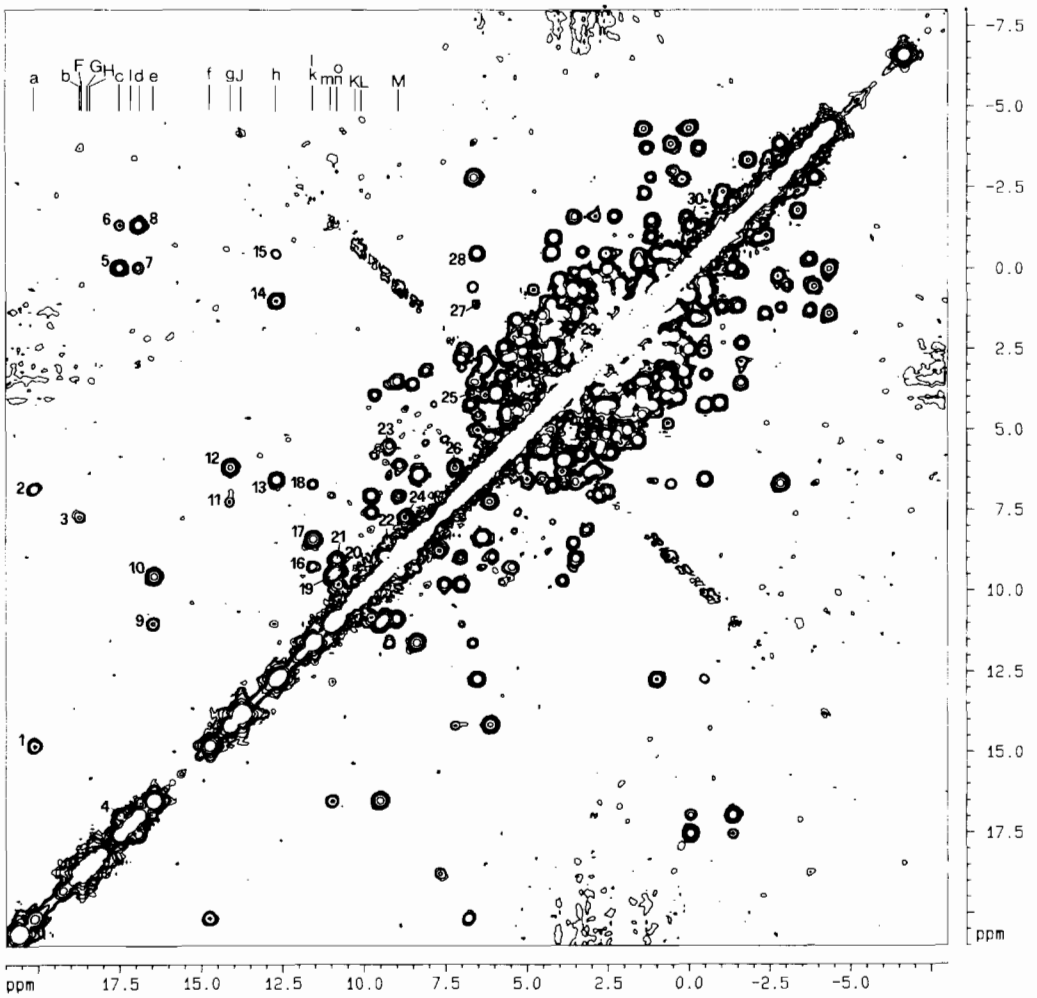

Fig. 4. Portion of the 400 MHz magnitude COSY map recorded using the same experimental conditions described for the NOESY spectrum. The downfield region containing the methyl peaks A, B, C, D, and E is omitted due to the absence of cross peaks.

TABLE 3. α-Methylene couples of heme propionate side chains detected by 1D-NOE, NOESY and COSY data in the ^{1}H NMR spectrum of oxidized cytochrome c_3 (Hildenborough)

Couple[a]	COSY cross peak	NOESY cross peak	NOE[b] (%)	Assignment
c,d	4	62	34	6- or 7-H_α heme II or III
h, 6.59	13	89	56	6-H_α heme IV
9.27, 5.42	23	106		7-H_α heme I
6.37, 3.93	25	113		7-H_α heme II or III
3.86, 1.55	29	118		6- or 7-H_α heme II or III

[a]ppm values are used when labelling is not available. [b]From 1D-NOE experiments when available.

nectivities showed by the other two-proton peak n,o indicate that one of the resonances is most probably a component of a histidine β-CH_2 group. Overall, seven of the eight β-CH_2–α-CH systems of the axial histidine have been identified. The fact that for some of them the α-CH proton exhibits a higher frequency than that of one of the β-CH_2 protons is a feature not uncommon in low-spin heme proteins [22, 51, 53].

Discussion

The dipolar and scalar connectivities among the hyperfine-shifted resonances in the ^{1}H NMR spectrum of the fully oxidized protein allowed the identification of the ring position of a number of heme methyl groups. However, only three of them (peaks H, I and J) could be assigned to individual hemes, in agreement with a

TABLE 4. β-CH_2 and α-CH proton resonances of the iron binding axial histidines detected by 1D-NOE, NOESY and COSY data in the ^1H NMR spectrum of oxidized cytochrome c_3 (Hildenborough)

β-CH_2 couple[a]	α-CH[a]	COSY (NOESY) β–β'	COSY (NOESY) β–α	COSY (NOESY) β'–α
a, f	6.85	1 (37)	2 (–)	–
b, 7.78	8.82	3 (40)	– (39)	24 (111)
e, 9.61	m	10 (73)	9 (72)	19 (99)
g, 6.18	7.28	12 (82)	11 (80)	26 (112)
k, 8.48	9.29	17 (97)	16 (96)	22 (104)
l, 6,75	9.29	18 (98)	16 (96)	– (105)
n, 9.48	8.94	20 (100)	21 (–)	– (103)

[a]ppm values are used when labeling is not available.

previous report [20], since the former two are involved in a short interheme contact known from the X-ray structure. Fan *et al.* [20] have reported an assignment of methyl resonances to individual hemes in *D.vulgaris* cytochrome c_3, (Miyazaki F) on the basis of the electron density distribution calculated from ^1H NMR saturation-transfer experiments performed on partially reduced samples. Comparison of this data with the results of the extensive NOE experiments described herein allow us to unravel the gross features of the crowded paramagnetic region of the spectrum. The two proteins from Miyazaki and Hildenborough strains show an 87% sequence homology, and the pattern of the hyperfine-shifted resonances is very similar. From the limited 1D-NOE experiments carried out by Fan *et al.* [20] it appears that the couples of methyl peaks A, H, and I, J in their labeling scheme correspond to the present peaks A, G and I, J, respectively. This leads to the clear correspondence of the peaks B and F in the two spectra. Moreover, peaks C, D, E of the Miyazaki protein should correspond to the same peaks in the Hildenborough protein, by noting in both cases the increased linewidth of signal E, and by consideration of the results described below. An illustrative scheme highlighting the relationships between the two spectral patterns is shown in Fig. 5 to facilitate discussion.

Fan *et al.* proposed that the group of four Miyazaki methyl resonances A, H, I, K belong to heme I. This assignment is consistent with our data since the present peaks A and G are known to correspond to an 8-CH_3 and 1-CH_3 group of the same heme, peak I to a 5-CH_3, and peak K can be assigned to a 3-CH_3 group. The methyl resonances of heme I can therefore be fully assigned, in agreement with the previous report. The assignment of peak A to a methyl group of heme I is supported by molecular modeling and NMR studies of the interaction of *D. vulgaris* cytochrome c_3 with rubredoxin and flavodoxin [7], and also by NMR experiments following partial oxidation of the reduced protein [15], which indicate that peak A should correspond to a methyl group of one of the least readily

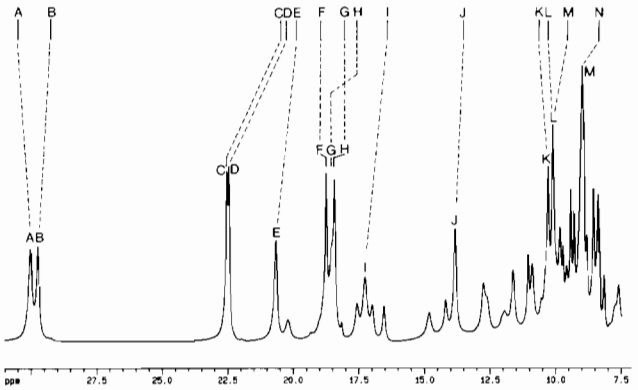

Fig. 5. Correspondence between the downfield shifted hyperfine resonances in the ^1H NMR spectra of oxidized *D. vulgaris* cytochrome, c_3, Hildenborough (below), and Miyazaki (above, from ref. 20).

oxidized hemes. Indeed heme I is proposed to have the highest reduction potential [20].

The Miyazaki methyl resonances C, D and J (corresponding to the same labeling in the present protein) were assigned to heme IV [20]. This agrees with the present data on the Hildenborough protein since peaks C and D can be assigned to the 5-CH_3 and 3-CH_3 group, respectively. The intermethyl connectivity of peak J (1-CH_3 of heme IV) with peak H then fixes the latter resonance as the 8-CH_3 group of the same heme. Peak H (G in the Miyazaki protein) was previously assigned to the 5-CH_3 group of heme III [18]. Two remaining groups of Miyazaki methyl resonances, each belonging to a distinct heme, namely B, F, G, M and E, L, N could not be assigned to individual hemes II and III [20]. With the exception of signal G (Miyazaki), labeled as H in our work with an assignment to heme IV, the present data are consistent with the idea that each of the above groups of resonances indeed arise from the same heme, but cannot provide assignments as detailed as above. In the former group, peaks B and F correspond to a 8-CH_3 and 1-CH_3 group, respectively; peak M could overlap with the other Miyazaki resonance L to give the present two-methyl peak L, and could cor-

respond to the 3-CH_3 group of the same heme. As far as the latter group E, L, N is concerned, E was assigned above to either a 8-CH_3 or 5-CH_3 group, L may correspond to the 3-CH_3 group and N, now M in the Hildenborough protein, may contain both the 5- or 8-CH_3 group and the 1-CH_3 group of the same heme. Overall, fifteen of the sixteen methyl resonances have been detected. The missing 5-CH_3 peak, belonging to heme II or III, is hidden in the diamagnetic region.

The group of broad resonances corresponding to seven to eight protons located between -10 and -25 ppm (Fig. 2) shows a shape and a spectral position characteristic of axial histidine ϵ-H protons in low spin ferric heme proteins [21, 25, 52, 54–59]. The integrated intensity fits with the presence of eight such protons from the eight axial histidines. Such correspondence is unlikely to be fortuitous. Some of these resonances were previously assigned to heme *meso*-CH resonances [44].

No hyperfine-shifted one-proton resonances assignable to δ-meso protons have been detected in the downfield region of the spectrum. The unassigned one-proton peaks, i, j, and o do not exhibit the required dipolar contacts with the 1- and 8-CH_3 groups, in either NOESY or 1D NOE experiments. On the other hand, several resonances, either falling in the diamagnetic region below 3 ppm, or upfield-shifted, were found to connect with the components of 1-CH_3, 8-CH_3 couples, and so the *δ-meso* protons may be among these resonances. Alternatively, these protons could be downfield shifted but their connectivities with the adjacent heme methyl groups may have not been detected due to their fast relaxation. The hyperfine shift of the *meso* protons in low-spin heme proteins is mainly dipolar in origin and, as demonstrated for *b*-type cytochromes [21], is strongly influenced by the orientation of the axial histidine(s). From crystallographic data the orientation is different for each of the four hemes in *D. vulgaris* cytochrome c_3 [3], and for at least two of them (hemes I and III) is consistent with the *δ-meso* proton being shifted upfield [21].

The hyperfine shift pattern of the methyl groups of the four hemes deserves some comment. It is known that the distribution of the unpaired spin density over the porphyrin ring is controlled by the chirality of the axial methionine in cytochrome *c* [43, 47, 60–63] and by the orientation of the imidazole plane of the axial histidine(s) in the other low spin hemes, such as those found in cytochrome *c* peroxidase, myoglobin and *b*-type cytochromes [21, 25, 50, 60, 64–66]. The proposed assignment of the methyl peaks of hemes I and IV (Table 1) may indicate that in cytochrome c_3 the orientation of the axial histidines still plays a role in determining the methyl shift pattern, even though the spin distributions of the individual hemes are likely to be complicated by cross interactions [3, 20]. Indeed, hemes I and IV, which are characterized by an almost perpendicular orientation of the histidine planes (in both hemes the axial imidazole groups are roughly coplanar) [3], display a pairwise inverted order of the chemical shift for the methyl groups: 8, 1, 5, 3 versus 5, 3, 8, 1 (in order of decreasing frequency), respectively. The lack of a firm assignment of the methyl groups to the individual hemes II and III prevents any further comparison. However, as far as the above fully assigned hemes are concerned, it appears that the heme methyl shift pattern in cytochrome c_3 differs from that commonly shown by *c*-type cytochromes characterized by the pairs 8, 3; 5, 1 or 5, 1; 8, 3 (in order of decreasing frequency) depending on the chirality of the axial methione [60].

Acknowledgements

High field ^{1}H NMR spectra were obtained at the Centro Grandi Strumenti of the University of Modena, Modena, Italy (400 MHz) and at the Ohio State University Campus Chemical Instrument Center (500 MHz). This work was supported by the NSF, grant number CHE-8921468. The Ministero della Ricerca Scientifica e Tecnologica of Italy is acknowledged for financial support.

References

1 J. LeGall, J. J. G. Moura, H. D. Peck and A. V. Xavier, in T. G. Spiro (ed.), *Iron–Sulfur Proteins,* Wiley, New York, 1982, p. 177.
2 T. Yagi, H. Inokuchi and K. Kimura, *Acc. Chem. Res., 16* (1983) 2.
3 Y. Higuchi, M. Kusunoki, Y. Matsuura, N. Yasuoka and M. Kakudo, *J. Mol. Biol., 172* (1984) 109.
4 R. Haser, M. Pierrot, M. Frei, F. Payan, J. P. Astier, M. Bruschi and J. LeGall, *Nature (London), 282* (1979) 806.
5 M. Pierrot, R. Haser, M. Frey, F. Payan and J. P. Astier, *J. Biol. Chem., 257* (1982) 14341.
6 D. E. Stewart, J. LeGall, I. Moura, J. J. G. Moura, H. D. Peck, A. V. Xavier, P. K. Weiner and J. E. Wampler, *Biochemistry, 27* (1988) 2444.
7 D. E. Stewart, J. LeGall, I. Moura, J. J. G. Moura, H. D. Peck, A. V. Xavier, P. K. Weiner and J. E. Wampler, *Eur. J. Biochem., 185* (1989) 695.
8 C. Cambillau, M. Frey, J. Mosse, F. Guerlesquin and M. Bruschi, *Protein Struct. Funct. Genet., 4* (1988) 63.
9 I. Bertini and C. Luchinat, *NMR of Paramagnetic Molecules in Biological Systems,* Benjamin/Cummings, Menlo Park, CA, 1986.
10 K. Fan, H. Akutsu, K. Niki, N. Higuchi and Y. Kyogoku, *J. Electroanal. Chem., 278* (1990) 295.
11 F. Guerlesquin, M. Noailly and M. Bruschi, *Biochem. Biophys. Res. Commun., 130* (1985) 1102.
12 H. Santos, J. J. G. Moura, I. Moura, J. LeGall and A. V. Xavier, *Eur. J. Biochem., 141* (1984) 283.

13 H. Santos, D. L. Turner and A. V. Xavier, *J. Magn. Reson., 59* (1984) 177.
14 J. J. G. Moura, A. V. Xavier, D. J. Cookson, G. R. Moore, R. J. P. Williams, M. Bruschi and J. LeGall, *FEBS Lett., 81* (1977) 275.
15 J. J. G. Moura, H. Santos, I. Moura, J. LeGall, G. R. Moore, R. J. P. Williams and A. V. Xavier, *Eur. J. Biochem., 127* (1982) 151.
16 A. V. Xavier and J. J. G. Moura, *Biochimie, 60* (1978) 327.
17 J. S. Park, M. Enoki, A. Ohbu, K. Fan, K. Niki and H. Akutsu, *J. Mol. Struct., 242* (1991) 343.
18 J. S. Park, K. Kano, K. Niki and H. Akutsu, *FEBS Lett., 285* (1991) 149.
19 K. Kimura, S. Nakajima, K. Niki and H. Inokuchi, *Bull. Chem. Soc. Jpn., 58* (1985) 1010.
20 K. Fan, H. Akutsu, Y. Kyogoku and K. Niki, *Biochemistry, 29* (1990) 2257.
21 S. J. McLachan, G. N. La Mar and K.-B. Lee, *Biochim. Biophys. Acta., 957* (1988) 430.
22 S. D. Emerson and G. N. La Mar, *Biochemistry, 29* (1990) 1545.
23 I. Bertini, F. Capozzi, C. Luchinat and P. Turano, *J. Magn. Reson., 95* (1991) 244.
24 L. Banci, I. Bertini, C. Luchinat, L. Messori and P. Turano, *J. Appl. Magn. Reson.,* in press.
25 J. Wu, G. N. La Mar, L. P. Yu, K. B. Lee, A. F. Walker, M. L. Chiu and S. G. Sligar, *Biochemistry, 30* (1991) 2156.
26 J. D. Satterlee and J. E. Erman, *Biochemistry, 30* (1991) 4398.
27 J. S. de Ropp and G. N. La Mar, *J. Am. Chem. Soc., 113* (1991) 4348.
28 L. Banci, I. Bertini, P. Turano, J. C. Ferrer and A. G. Mauk, *Inorg. Chem., 30* (1991) 4510.
29 L. Banci, I. Bertini, P. Turano, M. Tien and T. K. Kirk, *Proc. Natl. Acad. Sci. U.S.A., 88* (1991) 6956.
30 L. Banci, I. Bertini, P. Turano and M. Vicens Oliver, *Eur. J. Biochem., 204* (1992) 107.
31 G. N. La Mar, S. D. Emerson, J. T. J. Lecomte, U. Pande, K. M. Smith, G. W. Craig and L. A. Kehres, *J. Am. Chem. Soc., 108* (1986) 5568.
32 F. Guerlesquin, M. Bruschi and K. Wuthrich, *Biochim. Biophys. Acta, 830* (1985) 296.
33 F. Guerlesquin, M. Bruschi and G. Bovier-Lapierre, *Biochimie, 66* (1984) 93.
34 J. Tan and J. A. Cowan, *Biochemistry, 29* (1990) 4886.
35 T. Inubushi and E. D. Becker, *J. Magn. Reson., 51* (1983) 128.
36 L. Banci, I. Bertini, C. Luchinat and M. Piccioli, in I. Bertini, H. Molinari and N. Niccolai (eds.), *NMR and Biomolecular Structure,* VCH, Weinheim, 1991, p. 31.
37 L. Banci, I. Bertini, C. Luchinat, M. Piccioli, A. Scozzafava and P. Turano, *Inorg. Chem., 28* (1989) 4650.
38 I. Bertini, F. Briganti, C. Luchinat and A. Scozzafava, *Inorg. Chem., 29* (1990) 1874.
39 D. Neuhaus and M. Williamson, *The Nuclear Overhauser Effect in Structural and Conformational Analysis,* VCH, New York, 1989.
40 J. H. Noggle and R. E. Shirmer, *The Nuclear Overhauser Effect,* Academic Press, New York, 1971.
41 A. Kalk and J. J. C. Berendsren, *J. Magn. Reson., 24* (1976) 343.
42 J. Hockmann and H. Kellerhals, *J. Magn. Reson., 38* (1980) 23.
43 D. Marion and K. Wuthrich, *Biochem. Biophys. Res. Commun., 113* (1984) 967.
44 C. C. McDonald, W. D. Phillips and J. LeGall, *Biochemistry, 13* (1974) 1952.
45 T. Takano, *J. Mol. Biol., 110* (1977) 537.
46 R. M. Keller, A. Schejter and K. Wuthrich, *Biochim. Biophys. Acta, 626* (1980) 15.
47 H. Senn and K. Wuthrich, *Biochim. Biophys. Acta, 747* (1983) 16.
48 H. Senn, A. Eugster and K. Wuthrich, *Biochim. Biophys. Acta, 743* (1983) 58.
49 V. Thanabal, J. S. de Ropp and G. N. La Mar, *J. Am. Chem. Soc., 109* (1987) 7516.
50 S. D. Emerson and G. N. La Mar, *Biochemistry, 29* (1990) 1556.
51 G. R. Moore and G. Williams, *Biochim. Biophys. Acta, 788* (1984) 147.
52 J. S. de Ropp, G. N. La Mar, K. N. Smith and K. C. Langry, *J. Am. Chem. Soc., 106* (1984) 4438.
53 Y. Yamamoto, K. Iwafune, N. Nanai, A. Osawa, R. Chujo and T. Suzuki, *Eur. J. Biochem., 198* (1991) 299.
54 G. N. La Mar, P. D. Burns, J. T. Jackson, K. M. Smith, K. C. Langry and P. Strittmatter, *J. Biol. Chem., 256* (1981) 6075.
55 J. D. Satterlee, J. E. Erman, G. N. La Mar, K. M. Smith and K. C. Langry, *J. Am. Chem. Soc., 105* (1983) 2099.
56 J. D. Satterlee and J. E. Erman, *Biochim. Biophys. Acta, 743* (1983) 149.
57 J. D. Satterlee, J. E. Erman, J. M. Mauro and J. Kraut, *Biochemistry, 29* (1990) 8797.
58 S. Ramaprasad, R. D. Johnson and G. N. La Mar, *J. Am. Chem. Soc., 106* (1984) 5330.
59 G. N. La Mar, J. S. de Ropp, V. P. Chacko, J. D. Satterlee and J. E. Erman, *Biochim. Biophys. Acta, 708* (1982) 317.
60 J. D. Satterlee, *Annu. Rep. NMR Spectrosc., 17* (1986) 79, and refs. therein.
61 H. Senn and K. Wuthrich, *Q. Rev. Biophys., 18* (1985) 111.
62 H. Senn, F. Guerlesquin, M. Bruschi and K. Wuthrich, *Biochim. Biophys. Acta, 748* (1983) 194.
63 H. Senn and K. Wuthrich, *Biochim. Biophys. Acta, 746* (1983) 48.
64 G. N. La Mar and F. A. Walker, in D. Dolphin (ed.), *The Porphyrins,* Academic Press, New York, 1978.
65 R. G. Shulman, S. H. Glarum and M. Karplus, *J. Mol. Biol., 57* (1971) 93.
66 T. G. Traylor and A. P. Berzinis, *J. Am. Chem. Soc., 102* (1980) 2844.